WATER RESOURCES RESEARCH, VOL. 44, W11414, doi:10.1029/2008WR007033, 2008

Estimating transmissivity fields and their influence on flow and transport: The case of Champagne mounts

F. Renard[1] and N. Jeannée[2]

Received 21 March 2008; revised 21 July 2008; accepted 13 August 2008; published 12 November 2008.

[1] This paper presents a flexible and general methodology that combines hydrogeological and geostatistical modeling techniques to estimate a set of transmissivity fields and their influence on flow and transport. The methodology may be applied to any case with only hydraulic head observations, even if most of them are concentrated inside a small part of the entire domain of interest. It is applied here to the case of the Champagne chalk aquifer (France), where it is shown to be very efficient. The methodology is decomposed in three independent parts. First, a reference head distribution is constructed by kriging in order to constrain the inverse problem. As hydraulic heads and elevations are correlated, a smoothed digital elevation model is used as external drift. The inverse problem is then solved by using a simplified pilot point method with an efficient and easy-to-use minimization algorithm. Finally, geostatistical simulations combined with flow simulations lead to a set of acceptable transmissivity fields. The induced uncertainty is evaluated by calculating tracer concentrations, pointing out areas where flow behavior is uncertain and where new borings would be advantageously drilled.

Citation: Renard, F., and N. Jeannée (2008), Estimating transmissivity fields and their influence on flow and transport: The case of Champagne mounts, *Water Resour. Res.*, *44*, W11414, doi:10.1029/2008WR007033.

1. Introduction

[2] In many situations, the hydrogeology around a specific site has to be modeled without a good knowledge of the aquifer parameters. A very common difficulty is related to the small extent of the site area in comparison to the area of interest, which is defined by numerical and environmental considerations: boundary conditions of the flow involve water levels of rivers kilometers downstream of the site and the environmental impact of the site has to be estimated several kilometers away from its limits. Unfortunately, observations are often very difficult to obtain outside the site area, which represents sometimes only a few percent of the entire domain of interest.

[3] Estimating the transmissivity field on this extended area is of prime importance to estimate flow and dissolved compounds transport from the site to the hydrogeological outlets [*de Marsily et al.*, 2005]. However, even inside the site area, transmissivity observations are often missing, the different ways to measure transmissivity being costly, difficult to perform and interpret. Furthermore, the existing wells are rarely adapted for pumping tests, being too narrow or not deep enough. Actually they are often constructed only for environmental monitoring, groundwater chemical analyses or hydraulic head observations purposes. On the contrary, hydraulic head observations, easier to obtain, are commonly numerous, at least inside the site area.

[4] From a numerical point of view, since flow models derive water table elevation from the transmissivity knowledge, this leads to an inverse problem: determining a transmissivity field consistent with hydraulic head observations, with the help of a general knowledge of transmissivity behavior.

[5] In the case of poorly distributed head observations, it is good practice to first construct a reference head distribution on the entire domain of interest. This is usually done by kriging of the head observations [*Yeh et al.*, 1983]. If the topographic elevation or another auxiliary variable is correlated with the hydraulic head, cokriging or kriging with external drift can improve the head distribution [*Hoeksema et al.*, 1989; *Desbarats et al.*, 2002].

[6] As water table elevation is generally much smoother than topography [*Wolock and Price*, 1994], we first smooth the digital elevation model (DEM) and then use the smoothed topographic elevation as external drift. Among the multiple solutions to the inverse problem [*Yeh*, 1986; *de Marsily et al.*, 2000], we choose a simplified version of the pilot point method [*de Marsily*, 1978], combined with a simple and easy-to-use minimization algorithm avoiding gradient calculations. The pilot point method offers a flexible mean to obtain the precision required to solve the inverse problem by adjusting the pilot point density. This step leads to a reference transmissivity distribution.

[7] Sensitivity and uncertainty analysis of numerical models is commonly conducted on scalar parameters. Here, the impact of the spatial uncertainty of the transmissivity field on transport is assessed by using geostatistical simulations. Transmissivity fluctuations around the above reference transmissivity distribution are simulated. Each simulated transmissivity field is used in a steady state flow simulation, and the resulting hydraulic heads at observation points are compared with observed hydraulic heads. Only transmissivity fields leading to low errors are conserved,

[1]CEA, DIF, Arpajon, France.
[2]Geovariances, Avon, France.

0043-1397/08/2008WR007033$09.00

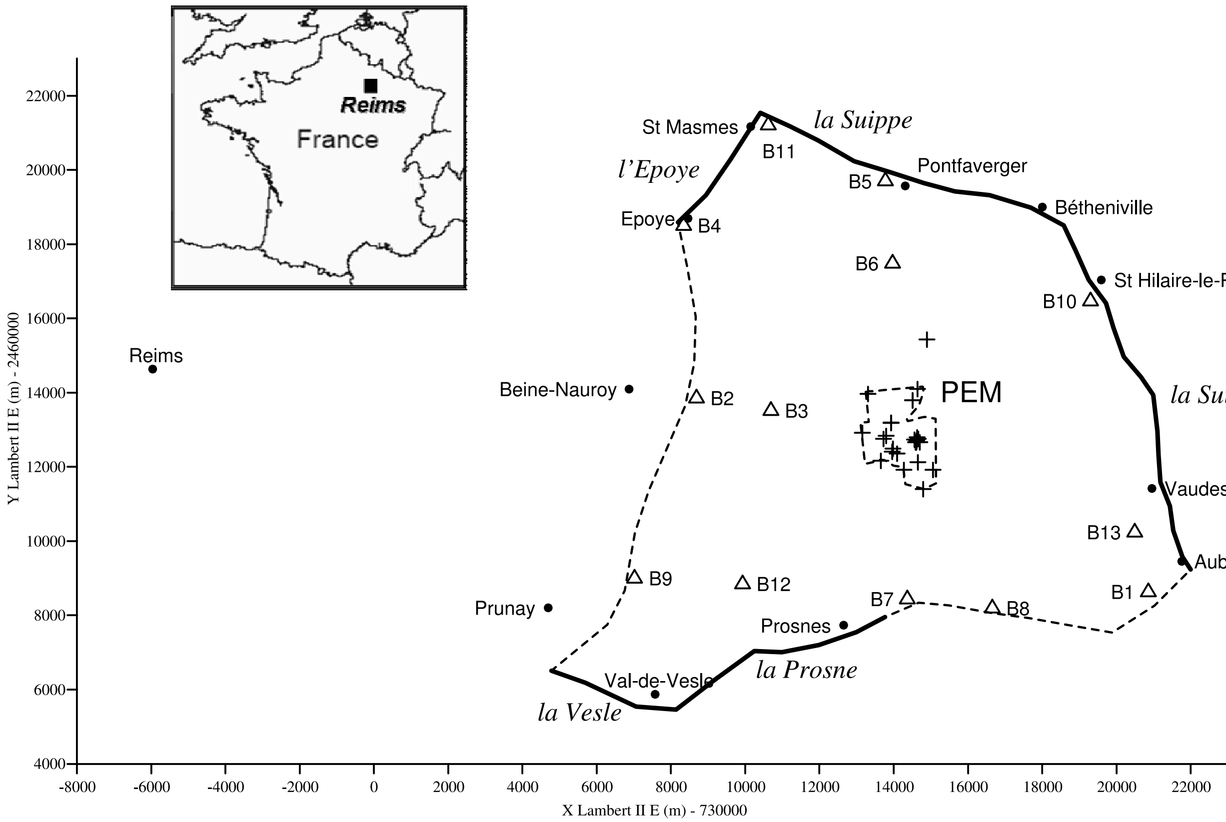

Figure 1. Domain of interest, PEM site, main rivers (solid lines), and towns (dots) and PEM (pluses; cf. Figure 2) and BRGM (triangles) observation points. In all maps, the origin is set to (730 km, 2460 km) in Lambert II extended coordinates, which corresponds to 49°7′29″N latitude and 4°6′59″E longitude.

and used for transport simulations. The resulting transport uncertainty is illustrated by calculating tracer concentrations.

[8] The three parts of this methodology, kriging, inverse problem and geostatistical simulations, are conceived to be fully independent, and there is no specification on the different grids to be used at each step, for the kriging, the flow and the geostatistical simulations. The proposed method for solving the inverse problem may be used without a prior kriging with external drift and even without any reference transmissivity field, the pilot points being in this case only the observation points. Also, the geostatistical simulations may be realized from any reference transmissivity field, not necessarily obtained by inversion.

[9] The methodology is applied to estimate transmissivity fields and flow around a site located in the Champagne chalk aquifer, about 20 km east of Reims, in the Marne department (France). Geostatistical and flow simulations are performed using ISATIS software [*Geovariances*, 2005] and METIS software in its bidimensional version [*Goblet*, 1989; *Cordier and Goblet*, 1999], respectively.

2. Material

2.1. Site Description

[10] The studied site is called the Polygone d'Expérimentation de Moronvilliers (PEM). It is located on the Champagne mounts, 20 km east of Reims (Marne, France). It is approximately 4 km^2 wide, in between the drainage divide of the Suippe and Vesle rivers (Figure 1). The domain of interest covers approximately 160 km^2 around the Champagne mounts. It is surrounded by several rivers: the Epoye, the Suippe and the Prosne (a tributary of the Vesle River) located in the north, the east and the south, respectively. It has been limited according to orthogonal lines to isoaltitudes, that represent approximately no flow boundaries. The aquifer is the Upper Cretaceous chalk. It lies within the white chalk of Campanian and Santonian ages, above the Turonian marly chalk [*Laurain et al.*, 1981; *Allouc and Le Roux*, 1995].

2.2. Hydraulic Head Data

[11] Hydraulic head data mainly come from piezometric observations performed in March 2005 on the 27 PEM wells (cf. Figures 1 and 2). Observations performed by the Bureau de Recherches Géologiques et Minières (BRGM) are available outside the site, thanks to a project aiming at modeling the hydraulic head level of the chalk groundwater in the Champagne-Ardennes region [*Rouxel-David*, 2003]. Among two campaigns performed by the BRGM, only the 13 observations of the April 2002 campaign have been kept, corresponding to high water levels consistent with the March 2005 campaign inside the PEM (cf. Figure 1). Both PEM (March 2005) and BRGM (April 2002) hydraulic head observations have been compared with long-time automatic head measurements and can be considered as mean values corresponding to quasi steady state conditions.

2.3. Model Definition

[12] The domain of interest is modeled by using a Voronoï type of mesh, consisting of 11345 nodes and 18943 triangular and quadrangular elements. The distance

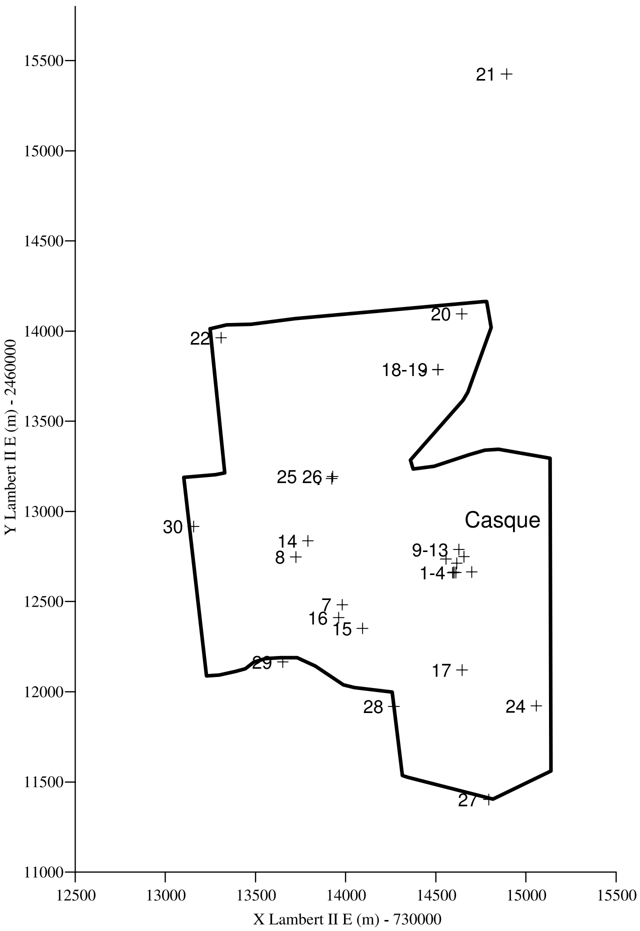

Figure 2. Location and name of PEM observation points.

between two nodes of a given element varies from 33 m to 409 m. The PEM area is covered by a 50 m regular square grid, identical to the digital elevation model.

[13] The boundary conditions for flow modeling are obtained by sampling elevations along the surrounding rivers (30 sampling points) and by interpolating between these points. The infiltration is set to 150 mm/a, according to data obtained from the Reims Meteo-France station. The chalk aquifer substratum is obtained by estimating the top of the C4C geological level, leading to a thickness of the aquifer varying from 0 to 80 m [*Laurain et al.*, 1981; *Allouc and Le Roux*, 1995].

3. Methodology

3.1. Definition of the Reference Hydraulic Head Distribution

[14] The appropriate way to model water table elevation depends on the spatial structure of hydraulic head data and on the potential existence of auxiliary data correlated with hydraulic heads observations. In the case of scarce clustered wells, kriging hydraulic head data alone would lead to an unrealistic water table elevation map. Kriging of hydraulic head observations with topographic elevation used as external drift is particularly appropriate in case of an existing correlation between both variables [*Desbarats et al.*, 2002].

[15] For each point x of the domain, kriging with external drift relies on the knowledge of a variable $s(x)$ linearly correlated with the variable of interest $Z(x)$. In case of high correlation, $s(x)$ provides a large-scale information about the spatial trend of $Z(x)$ and can be taken into account to estimate Z. Kriging with external drift only requires the knowledge of the variogram of the residuals from the regression of $Z(x)$ by $s(x)$ [*Chilès and Delfiner*, 1999].

[16] One of the earliest applications of this technique in hydrogeology consisted in mapping log transmissivity using specific capacity (log) as external drift [*Ahmed and de Marsily*, 1987]. *Chilès* [1991] applied this technique to map hydraulic heads for a given year using data from better sampled years.

[17] Using DEM as external drift usually provides unrealistic short-range fluctuations, as noted by *Wolock and Price* [1994, p. 3052]: "the water table configuration may be smoother than the land surface topography and may be related more accurately to a coarse resolution or map-scale DEM." Instead of decreasing the resolution of the DEM to create a coarse grid, we suggest to smooth the short-range fluctuations using a standard moving average algorithm. The smoothing radius is determined empirically, depending of the scale of the domain of interest and of the subjective satisfaction of the modeler. The smoothed topographic elevation map should be smooth enough to represent a hydraulic head distribution, but should conserve the main topographic characteristics. It will be set to 1000 m in the case of PEM.

[18] The hydraulic head distribution derived from this kriging using smoothed DEM as external drift is called the reference hydraulic head distribution. It is defined on the regular square grid used for kriging and will be used to solve the inverse problem.

3.2. Estimation of the Transmissivity Field

[19] Among the different techniques for solving the inverse problem, we choose to adapt the basic version of the pilot point method [*de Marsily*, 1978; *Certes and de Marsily*, 1991], which is simple and well suited to our problem.

3.2.1. Definition of Pilot Points

[20] The choice of the pilot points is not iterative nor optimized and only aims at covering uniformly the studied domain. In addition to the hydraulic head observations, pilot points are automatically selected among the mesh nodes used for the numeric flow simulation, in order to fill in the space left outside the observation points. The distance of each node to the closest observation point is calculated, and the node is considered as a pilot point if this distance exceeds a given threshold. More sophisticated methods could be used [*Ramarao et al.*, 1995; *Lavenue et al.*, 1995; *de Marsily et al.*, 2000] but are not appropriated given the low number of available data.

[21] At each additional point, the hydraulic head is then interpolated from the reference hydraulic head distribution obtained at the previous section. All the pilot points are given a transmissivity zone number ("pilot zone"), following their assumed similarity: geographic proximity, topographic similarity. Transmissivities are actually estimated for each zone and pilot points with the same zone number will therefore have the same transmissivity value. For each zone, minimum and maximum transmissivities have to be

defined. It is then possible to take into account actual transmissivity observations.

3.2.2. Minimization Algorithm

[22] The inverse problem reduces now to estimating the transmissivity values for each zone, that lead to the closest hydraulic head distribution to the reference one. It is solved by an iterative process that minimizes an error criterion, which is chosen here as the mean error over all pilot points:

$$e_i = \frac{1}{n}\sum_{k=1}^{n}\left|h_k^i - h_k^{ref}\right| \tag{1}$$

with n the total number of pilot points, h_k^i the calculated hydraulic head for point k at iteration i and h_k^{ref} the reference hydraulic head for point k.

[23] The mean error used here has the advantage to be directly understood as a mean hydraulic head deviation, independently of the number of pilot points, so that comparisons between calculations are easy. Any other error criterion such as the L2 norm could be used instead. Nevertheless, as the minimization algorithm avoids gradient calculations, the error criterion is used only as a stopping criterion, and the results are not dependent on this choice.

[24] This minimization problem can be solved by classical methods such as conjugate gradient combined with adjoint method for the gradients estimation. In our case where the error depends only on hydraulic heads, we use a simple and efficient algorithm based on a kind of steepest descent algorithm that avoids gradient calculations. The computational time is then noticeably reduced and very great numbers of pilot points may be used. This algorithm has been tested successfully on artificial problems where the reference hydraulic head fields are first generated from artificial transmissivity fields. In these cases, the algorithm has shown perfect convergence to these transmissivity fields.

[25] At each new iteration, the transmissivities values are calculated from

$$\begin{cases} T_j^{i+1} = (1+\alpha)T_j^i \ \mathit{if}\ \delta_j^i > 0 \\ T_j^{i+1} = (1-\alpha)T_j^i \ \mathit{if}\ \delta_j^i < 0 \end{cases} \tag{2}$$

with α strictly belonging to the interval]0, 1[, T_j^i the transmissivity for zone j at iteration i, δ_j^i the average difference for zone j between calculated and reference heads at iteration i:

$$\delta_j^i = \frac{1}{n_j}\sum_{k=1}^{n_j}\left(h_k^i - h_k^{ref}\right) \tag{3}$$

with n_j the number of pilot points in zone j.

[26] The parameter α is initially set to 0.5, which has been found to be a good compromise between precision and convergence speed. For each zone, transmissivity values are also constrained to lie between two bounds:

$$\forall i,j \quad T_j^{\min} \leq T_j^i \leq T_j^{\max} \tag{4}$$

[27] Starting from a set of transmissivity values for each zone, transmissivities are calculated at each element center of the grid used for flow simulations, using a classical inverse squared distance algorithm based on the closest neighbors. The resulting transmissivity field is used as input of a steady state flow simulation. The simulated hydraulic head distribution is interpolated to calculate the hydraulic heads at observation points, evaluate δ_j^i values and calculate the new values of transmissivities.

[28] The minimal error $e_{\min}$ is recorded during the iterative process, and the parameter α is divided by a factor 2 if the error increases too much: $e_i > \tau\, e_{\min}$, with τ set to 1.5. In this case, the iterative process is restarted from the iteration giving the minimal error. The iterative process is stopped if a maximum number of iterations is reached or if the error becomes smaller than a given limit $e_{\max}$: $e_i \leq e_{\max}$.

[29] This minimization process leads in a few tens of iterations to a set of transmissivity values for each zone, and then per interpolation to a transmissivity field over the entire domain. This field is defined on the grid used for flow simulations and is called the reference transmissivity field in the next sections.

3.3. Assessing the Uncertainty of the Transmissivity Field

[30] The reference transmissivity field relies on the hydraulic head observations (their value and location) and also on several parameters involved in the methodology: smoothing of the DEM, constraints on the authorized transmissivity intervals, choice of the sampling points for the hydraulic head distribution to reproduce, parameters of the optimization algorithm. Ignoring these uncertainties can lead to significant errors during transport modeling.

[31] Here, the uncertainty of the transmissivity field is assessed by means of geostatistical simulations combined with flow simulations. The approach consists in generating a set of acceptable transmissivity fields, using geostatistical simulations, and then to simulate the related hydraulic head distributions using steady state flow simulation. The quality of each transmissivity field is evaluated by comparison between the simulated and the observed hydraulic heads.

[32] In order to constrain the uncertainty of simulations with geologically acceptable distributions, the reference transmissivity field (obtained by inverse optimization) is used as an a priori distribution. A set of transmissivity fields is then obtained by simulating fluctuations around this reference distribution:

$$\ln T_i(x) = \ln T_0(x) + D(x)R(x) \tag{5}$$

with x a mesh center, T_0 the reference transmissivity value, T_i the transmissivity value for simulation i, R a multi-Gaussian residual, D a dispersion term for the residuals used to control the confidence in the reference transmissivity field.

[33] Gaussian residuals are simulated using the turning bands algorithm [*Matheron*, 1973; *Chilès and Delfiner*, 1999]. Given the absence of transmissivity observations, the spatial structure of these residuals can only be chosen using a heuristic approach, relying on the plausibility of the resulting transmissivity simulations.

[34] A steady state flow simulation using METIS produces a hydraulic head distribution for each input transmis-

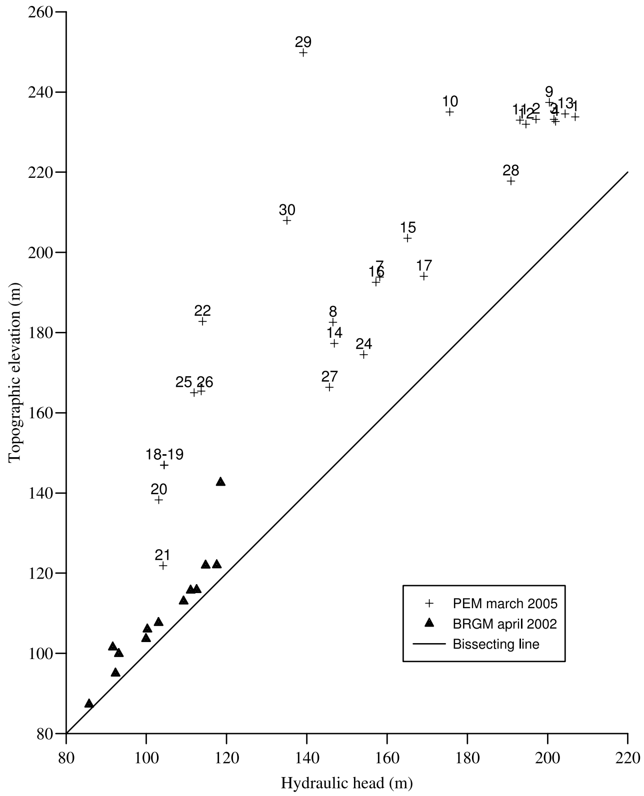

Figure 3. Hydraulic head versus elevation at observation points. The numbers of PEM borings are indicated.

sivity field. The quality of the simulated transmissivity fields is measured by the mean error:

$$e = \frac{1}{n_{obs}} \sum_{k=1}^{n_{obs}} \left| h_{sim}^{k} - h_{obs}^{k} \right| \tag{6}$$

with n_{obs} the number of observation points, h_{sim} et h_{obs} the simulated and the observed hydraulic heads at observation points, respectively. Transmissivity fields leading to too high errors are eliminated.

[35] In order to control the general behavior of the generated transmissivity fields, a weighted mean transmissivity field may be derived from the simulations:

$$\ln T = \frac{1}{\sum_{i=1}^{n_s} \frac{1}{e_i}} \sum_{i=1}^{n_s} \frac{\ln T_i}{e_i} \tag{7}$$

with n_s the number of selected simulations and e_i the error (equation (6)) of simulation i.

[36] Again, the hydraulic head error (equation (6)) may be computed on this average distribution. If the reference distribution has been correctly optimized, the average transmissivity field is expected to give similar or slightly higher errors, which would validate the reference distribution. On the contrary, the procedure will be used to put into evidence a more satisfying configuration of transmissivity values. Furthermore, the set of selected transmissivity fields can be used to evaluate the induced uncertainty on transport modeling.

4. Results and Discussion

4.1. Reference Hydraulic Head Distribution

[37] Figure 3 presents hydraulic head versus topographic elevation of the 40 observation points included in the area of interest. It shows a global correlation between both variables, that justifies the use of kriging of hydraulic heads with DEM as external drift. Nevertheless, two trends can be observed, reflecting two different hydrogeological behaviors, that are related to the stratigraphic position of the water table within the Chalk of Campanian versus Santonian age. Piezometer A29 presents a very low hydraulic head that could indicate a locally karstic behavior, resulting from a local cover of clay as evidenced by *Maurice et al.* [2006] in a similar aquifer.

[38] A DEM smoothing with a radius of 1000 m gives the topographic map of Figure 4a. Higher smoothing radius would erase the main topographic characteristics, and lower radius would lead to unrealistic uneven water level surface.

[39] A hydraulic head variogram model is fitted to the experimental variogram deduced from the observation data only. It uses an isotropic spherical model with range 1470 m and sill 1300 m^2, without nugget effect.

[40] The hydraulic head distribution obtained from kriging with external drift is shown in Figure 4b and is called the reference hydraulic head distribution. For a few points close to the rivers surrounding the domain, the estimated hydraulic head is slightly higher than the topographic elevation. In these cases, the hydraulic head is set to the topographic elevation.

4.2. Transmissivity Field Estimation

[41] The construction of the transmissivity field is based on the calculation of transmissivities at each "pilot zone". These zones include the 40 head observation points: 27 points inside the 4 km^2 of PEM, and 13 points outside. Some of the 27 PEM points are very close and are naturally grouped into 14 different zones (see Figure 7). The 13 BRGM points are distant enough to define 13 different zones. The zone densities are 4 and 0.1 points/km^2, respectively.

[42] In order to compensate this difference and to reproduce correctly the reference hydraulic head distribution (Figure 4b) on the entire domain, it is necessary to add pilot points outside the PEM limits. The greater the number of pilot points, the closer the hydraulic head distribution from the reference one. As the minimization algorithm does not need gradient calculations, the number of pilot points can be very large. In order to best reproduce the reference hydraulic head distribution, a maximal distance between two pilot points of 50 m is chosen, consistent with the model mesh definition. This leads to 8882 additional points. Therefore, the total number of pilot points is 8922, corresponding to 8909 zones.

[43] Initial, minimum and maximum transmissivities are chosen to be 4.10^{-4}, 10^{-7} and 4.10^{-1} m^2/s, respectively, in order to cover the entire range of known chalk transmissivities in the area [*Crampon et al.*, 1993, section 2.4], as well as values determined locally.

[44] The algorithm of section 3.2 is then applied in order to estimate transmissivities at each pilot point, and then at

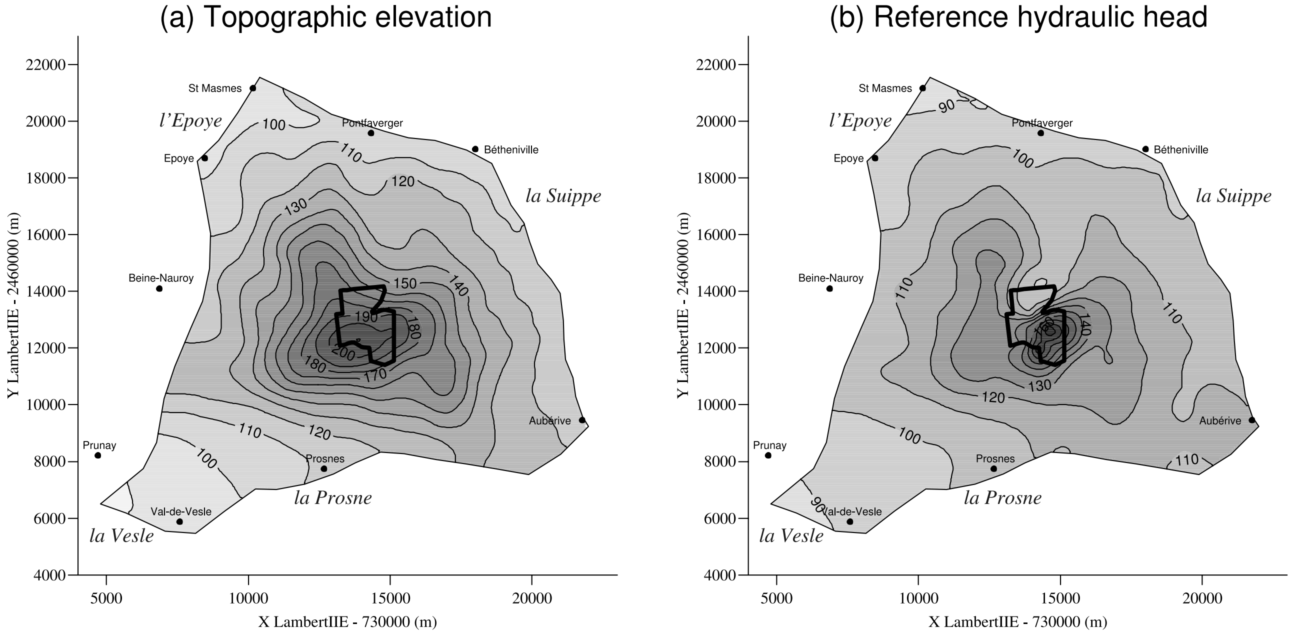

Figure 4. (a) Topographic elevation contour map (m) obtained from DEM smoothing with smoothing radius 1000 m. (b) Reference hydraulic head contour map (m) obtained from kriging of hydraulic head data with the smoothed DEM as external drift.

each node by interpolation. The results are obtained in a few tens of iterations (see Figure 5). Figures 6a and 6b show the resulting transmissivity and hydraulic head distributions. Figure 7 shows the calculated transmissivity values at PEM observation points and Figure 8 compares the calculated and measured hydraulic heads at observation points. Average hydraulic head errors are reported in Table 1, according to equation (1) and for different groups of points.

[45] Calculated hydraulic heads are globally very close to the measured heads, discrepancies being generally very small. They correspond to two main cases. (1) Calculated transmissivity equal to the maximum allowed transmissivity. It is the case for piezometers A18, A19, A20 and A21, located in the main valley descending from the PEM mounts, and where hydraulic heads are very low. (2) Discrepancies can occur for groups of points with inconsistent measured heads. It is essentially the case for zone 1, that groups the 9 piezometers located on the mount called Le Casque (cf. Figure 2). The hydraulic heads of these piezometers vary from 193 to 207 m, and these levels cannot be obtained with only one transmissivity value.

4.3. Geostatistical Transmissivity Simulations

[46] The uncertainty of the preceding transmissivity field is now assessed by means of geostatistical simulations. The dispersion term D of equation (5) is constructed in order to modify transmissivities at each grid cell by a factor 0.1 to 10, with confidence interval 95% (that is 1.96σ). In terms of log transmissivities, the value of this dispersion term is $\ln(10)/1.96 = 1.17$. The range of the transmissivity variation factor (0.1 to 10) is chosen in order to cover the general uncertainty on transmissivity measurements. It is not of first importance because transmissivity fields leading to too high hydraulic head error (cf. equation (6)) will be eliminated. The goal is to obtain a sufficient number of acceptable transmissivity fields representing the plausible fluctuations around the reference transmissivity field.

[47] Two thousand nonconditional simulations of gaussian residuals have been performed using the turning bands method (2500 bands). The number of simulations is chosen in order to keep a sufficient number of transmissivity fields once eliminated those which poorly reproduce the hydraulic head distribution.

[48] The transmissivity fields are generated directly from equation (5), and with the constraint on transmissivities to vary between 10^{-7} and 4.10^{-1} m^2/s. Sensitivity analysis has been conducted for the choice of the variogram models for the gaussian residuals R: several output simulations have been reviewed for their hydrogeological relevance, regarding the spatial uncertainty of the transmissivity field. Finally,

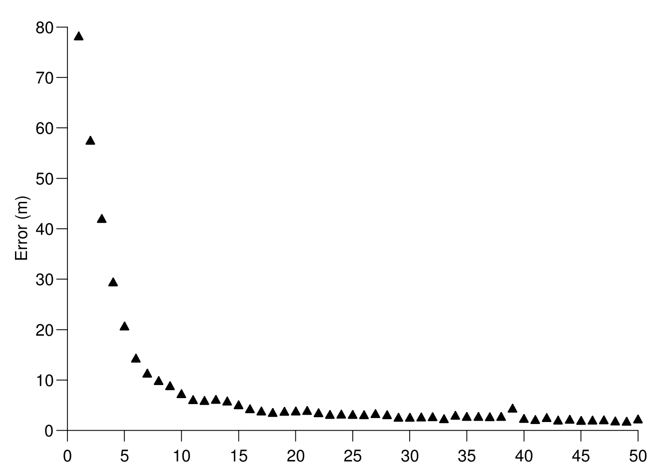

Figure 5. Error between calculated and reference hydraulic head at pilot points versus iteration number.

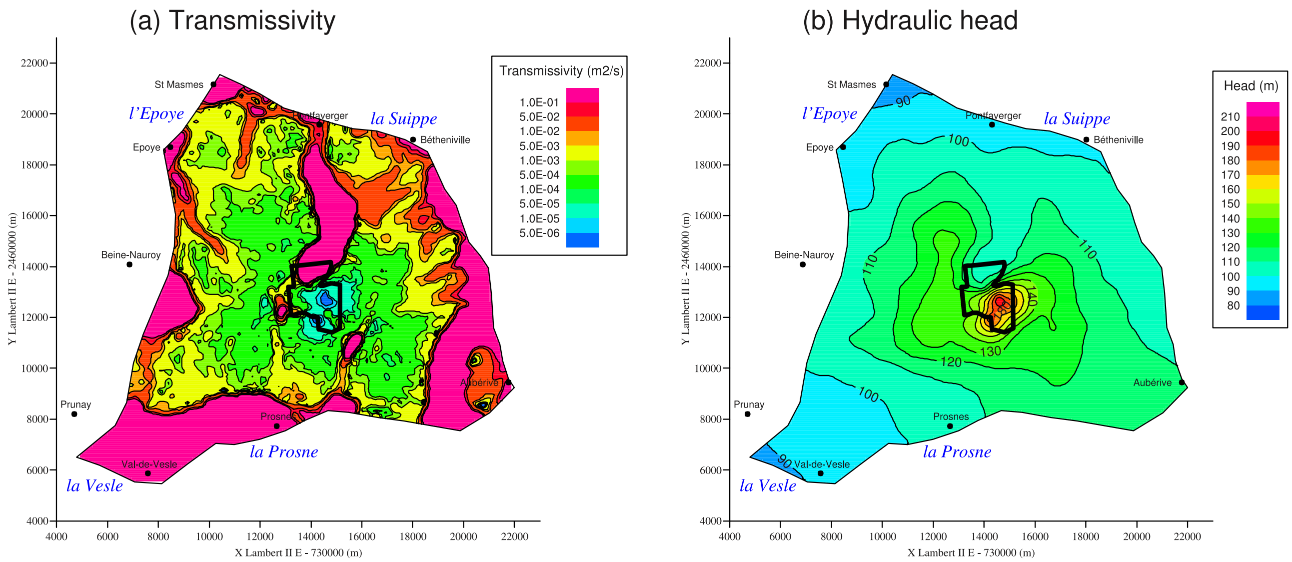

Figure 6. (a) Transmissivity field obtained by inversion algorithm. (b) Hydraulic head distribution obtained by steady state flow simulation from the inverse transmissivity field. This hydraulic head distribution is very similar to the one of Figure 4b.

a cubic variogram with range 2000 m is chosen for the gaussian residuals *R*, in order to have small uncertainty at small distances and a globally smooth behavior of residuals.

[49] In order to eliminate poor quality transmissivity fields, only 834 simulations are retained, that produce a hydraulic head error (cf. equation (6)) less than 10 m. This cutoff value is the maximal standard deviation calculated on a series of hydraulic head measurements at the different PEM piezometers. From these simulated transmissivity fields, a weighted mean transmissivity field is obtained according to equation (7). Table 2 presents the corresponding hydraulic head errors at observation points. As expected, the total hydraulic head error at observation points, 4.32 m, is larger that the same error obtained by direct optimization: 1.50 m. While hydraulic head errors at BRGM measurement points are similar for both distributions, the errors at PEM measurement points are appreciably higher with the geostatistical method. This comes very likely from scale and mesh effects, PEM area being only 2.5% of the total studied area, with complicated topography and several observation points, while BRGM points are situated on smoother areas with smaller density. Improving these results would require a specific analysis of the PEM area with a refined mesh and probably a different treatment of the head variogram.

4.4. Tracer Concentration Estimations

[50] One of the main interests of the approach is the possibility to evaluate the uncertainty induced by the uncertainty of the transmissivity field on concentrations.

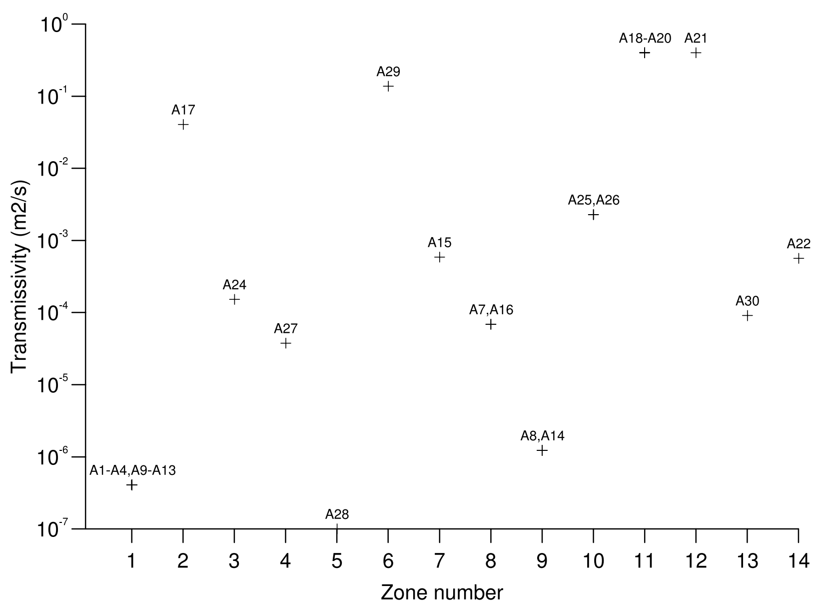

Figure 7. Transmissivity values at PEM observation points, organized by zone number.

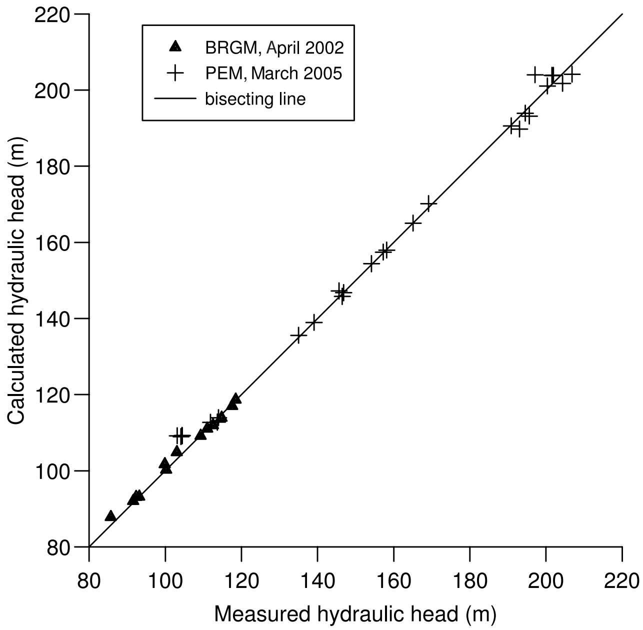

Figure 8. Calculated and measured hydraulic heads at observation points.

This is illustrated by the transport of a tracer injected at the center of PEM. In this study, the unsaturated zone is not taken into account and the tracer is supposed to be directly injected in the groundwater. The injection is done at a constant unit concentration during 10 years and on a surface of 10000 m^2.

[51] Figures 9a, 9b, and 9c show the maximum values over time of the tracer concentrations on the entire domain in three different cases. (1) Reference transmissivity field is used (Figure 9a). (2) Weighted mean transmissivity field from geostatistical simulations is used (Figure 9b). (3) The mean value of concentrations is calculated at each node from the 834 selected transmissivity fields used in transport calculations (Figure 9c).

[52] The tracer concentration distributions are very similar in the two first cases but the third one shows clearly two possible flow directions, to the west and to the south, that do not appear in the other cases. This indicates an important uncertainty on the flow in these directions.

[53] The geostatistical simulations enable also to evaluate other statistical results, such as risk evaluations and confidence intervals estimations. This is illustrated by Figures 10 and 11.

[54] Figure 10 shows the probability for the tracer concentrations to be greater than 1% of the initial unit concentration, by taking into account the 834 transmissivity fields obtained by geostatistical simulations. The plausible flow directions to the west and to the south appear also clearly here. This indicates a lack of information in these areas and leads to consider new borings there, with hydraulic head and transmissivity measurements.

[55] Figure 11 shows the tracer concentrations versus time at different points: piezometers A20 and A22, and two points called AUX2 and AUX4, located in the west and southwest area of PEM (see Figure 10), respectively. It illustrates how the information coming from the geostatistical simulations can be used, by calculating confidence intervals and statistical values. In this case, the uncertainty on transmissivity field can lead to important uncertainties on the tracer concentration and on the time of the peak's arrival. The uncertainties are particularly high in the case of points AUX2 and AUX4, that confirms the high uncertainty on flow in the west and southwest area of PEM.

Table 1. Hydraulic Head Errors for Different Groups of Points in the Case of the Reference Transmissivity Field[a]

Pilot	PEM and BRGM	PEM	BRGM	Additional Points
0.61	1.50	1.89	0.70	0.61

[a]Pilot points error is computed for all pilot points and is used for the optimization process. Error is given in meters.

5. Conclusion

[56] Hydrogeological modeling has to face a lot of choices when dealing with real cases, from the methods to be used to the assumptions to be done. Estimating the transmissivity field and its uncertainty constitutes one of the main issues to be solved. The present methodology gives directions to address this problem, from the processing of scarce and poorly distributed hydraulic head observations to the evaluation of the uncertainties induced by transmissivities on transport modeling. One of its main practical applications is the identification of areas where flow behavior is uncertain, and where new borings will be advantageously drilled. It has been successfully applied to the case of Champagne mounts.

[57] The methodology can be decomposed into three independent parts, each of them containing a specific development. (1) The correlation observed between topography and hydraulic head is used to construct a reference hydraulic head field by means of kriging with external drift approach. This drift comes from a prior smoothing of the digital elevation model. (2) A simple and robust minimization algorithm based on the steepest descent method combined with a modified version of the pilot point method allows for efficiently solving the inverse problem and produce a reference transmissivity field. (3) Geostatistical simulations are performed to generate a set of plausible transmissivity fields, that are used to evaluate the uncertainties on transport calculations.

[58] The approach is flexible and general enough to be applied to most real cases. It authorizes the use of any type of grid at each step, and gives the modeler the necessary parameters to deal with his specific case and control the

Table 2. Hydraulic Head Errors at PEM and BRGM Observation Points in the Case of the Weighted Mean Transmissivity Field Obtained From Geostatistical Simulations[a]

PEM and BRGM	PEM	BRGM
4.32	5.95	0.94

[a]Error is given in meters.

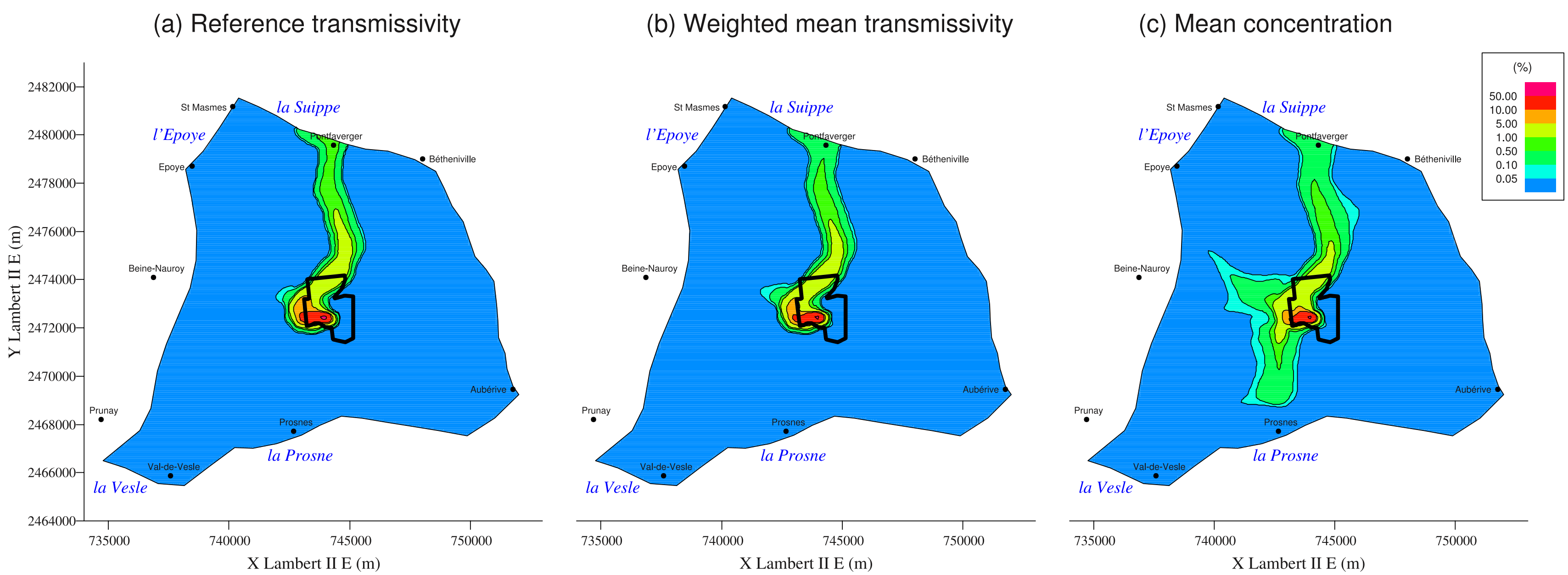

Figure 9. Maximum value over time of tracer concentrations (in percent of the initial unit concentration) obtained from three different methods. (a) Reference transmissivity field from direct optimization is used. (b) Weighted mean transmissivity field from geostatistical simulations is used. (c) The mean value of concentrations is calculated at each node from the 834 selected transmissivity fields used in transport calculations.

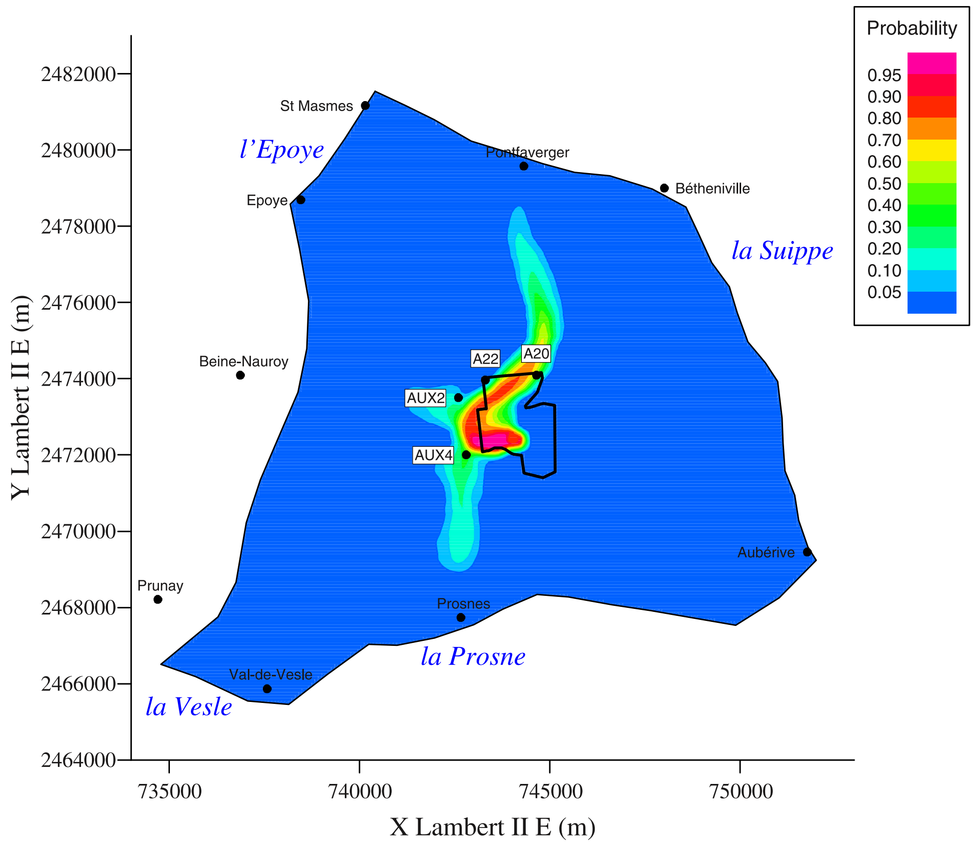

Figure 10. Probability for the tracer concentration to be greater than 1% of the initial concentration. The tracer concentrations at points A20, A22, AUX2, and AUX4 are shown in Figure 11.

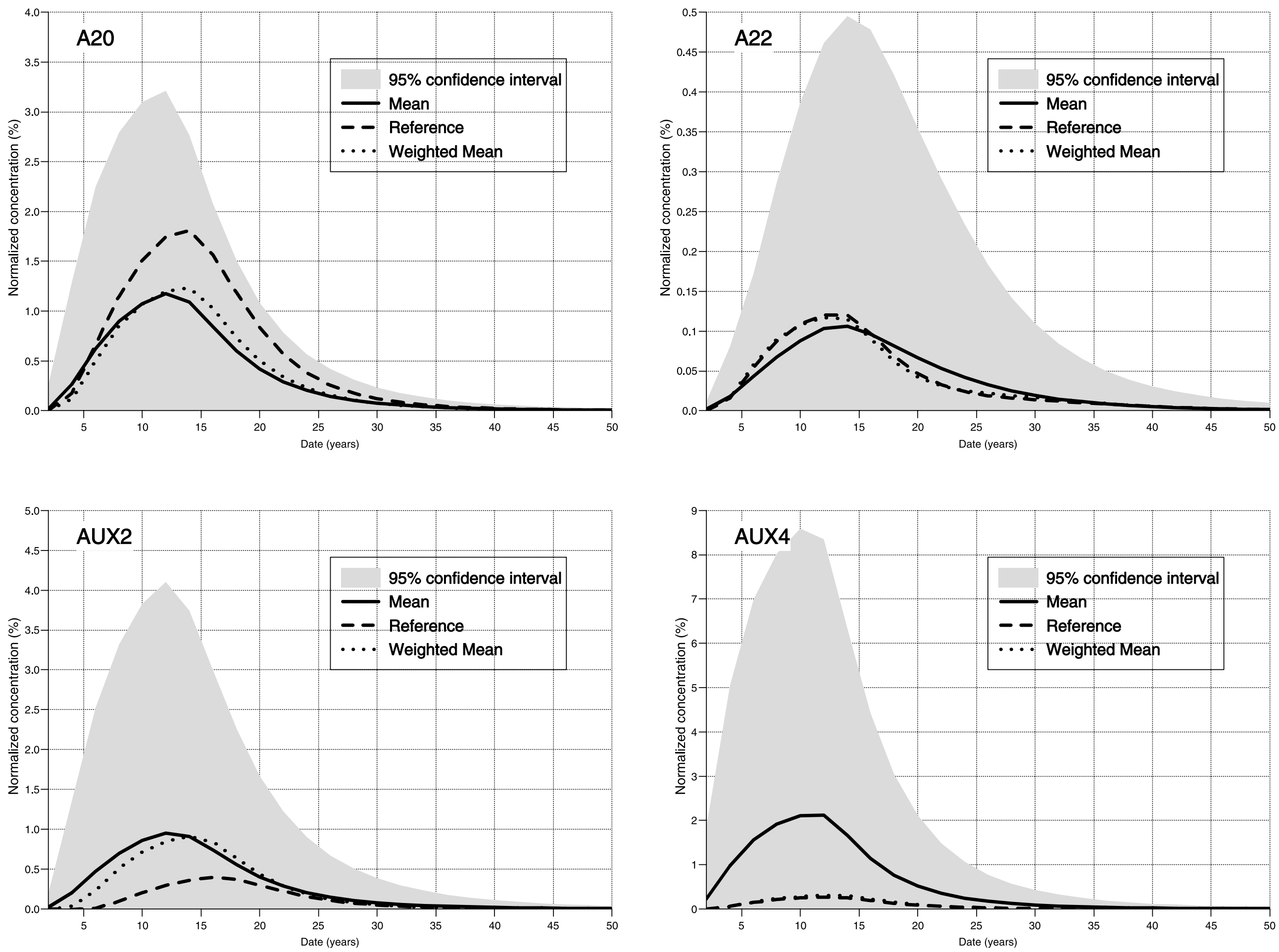

Figure 11. Tracer concentrations versus time at points A20, A22, AUX2, and AUX4 (see locations in Figure 10). The gray part shows the 95% confidence interval from the 834 selected transmissivity fields. The solid line is the tracer concentration obtained by calculating the mean value of concentrations from the 834 selected transmissivity fields. The dashed line is obtained by transport calculation using the reference transmissivity field. The dotted line is obtained by transport calculation using the weighted mean transmissivity field from geostatistical simulations.

assumptions throughout the process. The approach can next be combined with a classical uncertainty evaluation induced by uncertainties on scalar transport parameters, in order to construct a general scheme of uncertainty analysis.

[59] **Acknowledgments.** The authors would like to thank Nicolas Flipo, Ghislain de Marsily, Delphine Patriarche, Eric Pili, and three anonymous reviewers for their fruitful comments and corrections on the preliminary versions of the manuscript.

References

Ahmed, S., and G. de Marsily (1987), Comparison of geostatistical methods for estimating transmissivity using data on transmissivity and specific capacity, *Water Resour. Res.*, *23*(9), 1717–1737.

Allouc, J., and J. Le Roux (1995), Carte géologique de France (1/50000), feuille Mourmelon-le-Grand (133), notice explicative, Bur. de Rech. Geol. et Min., Orleans, France.

Certes, C., and G. de Marsily (1991), Application of the pilot point method to the identification of aquifer transmissivities, *Adv. Water Resour.*, *14*(5), 284–300.

Chilès, J. (1991), Application du krigeage avec dérive externe l'implantation d'un réseau de mesures piézométriques, *Sci. Terre*, *30*, 131–147.

Chilès, J., and P. Delfiner (1999), *Geostatistics: Modeling Spatial Uncertainty*, John Wiley, New York.

Cordier, E., and P. Goblet (1999), Programme Metis. Simulation d'écoulement et de transport miscible en milieu poreux et fracturé, notice d'emploi, *Tech. Rep. LHM/RD/99/18*, Ecole des Min. de Paris, Paris.

Crampon, N., J.-C. Roux, and P. Bracq (1993), Hydrogéologie de la craie en France, *Hydrogeologie*, *2*, 81–123.

de Marsily, G. (1978), De l'identification des systèmes hydrologiques, Ph.D. thesis, Univ. Paris VI, Paris.

de Marsily, G., J. Delhomme, A. Coudrain-Ribstein, and A. Lavenue (2000), Four decades of inverse problems in hydrogeology, *Spec. Pap. 348*, pp. 1–17, Geol. Soc. of Am., Boulder, Colo.

de Marsily, G., F. Delay, J. Goncalves, P. Renard, V. Teles, and S. Violette (2005), Dealing with spatial heterogeneity, *Hydrogeol. J.*, *13*, 161–183.

Desbarats, A., C. Logan, M. Hinton, and D. Sharpe (2002), On the kriging of water table elevations using collateral information from a digital elevation model, *J. Hydrol.*, *255*, 25–38.

Geovariances (2005), Isatis technical references, version 5, Ecole des Min. de Paris, Paris.

Goblet, P. (1989), Programme Metis. Simulation d'écoulement et de transport miscible en milieu poreux et fracturé, notice de conception, *Tech. Rep. LHM/RD/89/23*, Ecole des Min. de Paris, Paris.

Hoeksema, R., R. Clapp, A. Thomas, A. Hunley, N. Farrow, and K. Dearstone (1989), Cokriging model for estimation of water table elevation, *Water Resour. Res.*, *25*(3), 429–438.

Laurain, M., H. Guérin, and R. Durand (1981), Carte géologique de France (1/50000), feuille Reims (132), notice explicative, Bur. de Rech. Geol. et Min., Orleans, France.

Lavenue, A., B. Ramarao, G. de Marsily, and M. Marietta (1995), Pilot point methodology for automated calibration of an ensemble of conditionally simulated transmissivity fields: 2. Application, *Water Resour. Res.*, *31*(3), 495–516.

Matheron, G. (1973), The intrinsic random functions and their applications, *Adv. Appl. Probab.*, *5*, 439–468.

Maurice, L., T. Atkinson, J. Barker, J. Bloomfield, A. Farrant, and A. Williams (2006), Karstic behaviour of groundwater in the English chalk, *J. Hydrol.*, *330*(1–2), 63–70, doi:10.1016/j.jhydrol.2006.04.012.

Ramarao, B., A. Lavenue, G. de Marsily, and M. Marietta (1995), Pilot point methodology for automated calibration of an ensemble of conditionally simulated transmissivity fields: 1. Theory and computational experiments, *Water Resour. Res.*, *31*(3), 475–493.

Rouxel-David, E. (2003), Cartographie de la piézométrie de la nappe de la craie en Champagne-Ardenne, rapport final, *Tech. Rep. BRGM/RP-52332-FR*, Bur. de Rech. Geol. et Min., Orleans, France.

Wolock, D., and C. Price (1994), Effects of digital elevation model map scale and data resolution on a topography-based watershed model, *Water Resour. Res.*, *30*(11), 3041–3052.

Yeh, W.-G. (1986), Review of parameter identification procedures in groundwater hydrology: The inverse problem, *Water Resour. Res.*, *22*(2), 95–108.

Yeh, W.-G., Y. Yoon, and K. Lee (1983), Aquifer parameter identification with kriging and optimum parameterization, *Water Resour. Res.*, *19*(1), 225–233.

N. Jeannée, Geovariances, 49 bis avenue F. Roosevelt, BP 91, F-77212 Avon, France. (jeannee@geovariances.com)

F. Renard, CEA, DIF, F-91297 Arpajon, France. (francois.renard@cea.fr)